Supplementary Information for "Normal stress anisotropy and marginal stability in athermal elastic networks"

Jordan Shivers,[1,2] Jingchen Feng,[2] Abhinav Sharma,[3] and F. C. MacKintosh[1,2,4]

[1]*Department of Chemical and Biomolecular Engineering, Rice University, Houston, TX 77005, USA*
[2]*Center for Theoretical Biological Physics, Rice University, Houston, TX 77030, USA*
[3]*Leibniz-Institut für Polymerforschung Dresden, 01069 Dresden, Germany*
[4]*Departments of Chemistry and Physics & Astronomy, Rice University, Houston, TX 77005, USA*

Affinely deforming isotropic network models

Consider a filament segment with initial orientation $\hat{\mathbf{n}}$, undergoing deformation described by the tensor $\mathbf{\Lambda}(\gamma)$. The deformation changes the filament's length and orientation, resulting in a tension $\boldsymbol{\tau}$ directed along its new orientation. Treating the filament as a linear elastic element with stretching modulus μ and initial length $l_0 = 1$, the tension vector is $\boldsymbol{\tau} = \tau\mathbf{\Lambda}\hat{\mathbf{n}}/|\mathbf{\Lambda}\hat{\mathbf{n}}|$. For the spring model, we utilize a linear Hookean force-extension relation in which the filaments support both tension and compression: $\tau = \tau_s$ where $\tau_s = \mu(|\mathbf{\Lambda}\hat{\mathbf{n}}| - 1)$. For the rope model, we instead use a one-sided force-extension relation that is only finite under tension: $\tau = \tau_r$, with

$$\tau_r = \begin{cases} \mu(|\mathbf{\Lambda}\hat{\mathbf{n}}| - 1) & (|\mathbf{\Lambda}\hat{\mathbf{n}}| > 1) \\ 0 & (|\mathbf{\Lambda}\hat{\mathbf{n}}| \leq 1) \end{cases}. \tag{1}$$

Taking the average, over all initial filament orientations, of the product of the i component of the tension, $\tau\Lambda_{il}n_l/|\mathbf{\Lambda}\hat{\mathbf{n}}|$, and the line density of filaments crossing the j plane after the deformation, $\frac{\rho}{\det\mathbf{\Lambda}}\Lambda_{jk}n_k$, yields the stress tensor [1, 2],

$$\sigma_{ij} = \frac{\rho}{\det\mathbf{\Lambda}}\left\langle \tau\frac{\Lambda_{il}n_l\Lambda_{jk}n_k}{|\mathbf{\Lambda}\hat{\mathbf{n}}|}\right\rangle. \tag{2}$$

Since we consider only volume-conserving simple shear, $\det\mathbf{\Lambda} = 1$. Thus, for filaments in 3D with initial polar angle θ and azimuthal angle φ, the stress tensor is

$$\sigma_{ij} = \frac{\rho}{4\pi}\int_\varphi\int_\theta d\theta d\varphi \sin\theta\left[\tau\frac{\Lambda_{il}n_l\Lambda_{jk}n_k}{|\mathbf{\Lambda}\hat{\mathbf{n}}|}\right], \tag{3}$$

in which the deformation tensor for simple shear in 3D is

$$\mathbf{\Lambda}(\gamma) = \begin{pmatrix} 1 & 0 & \gamma \\ 0 & 1 & 0 \\ 0 & 0 & 1 \end{pmatrix} \tag{4}$$

and the transformed orientation vector is

$$\mathbf{\Lambda}\hat{\mathbf{n}} = \begin{pmatrix} \sin\theta\cos\varphi + \gamma\cos\theta \\ \sin\theta\sin\varphi \\ \cos\theta \end{pmatrix}. \tag{5}$$

We compute the *xz*, *xx*, and *zz* components of the stress tensor for the 3D case as follows:

$$\sigma_{xz} = \frac{\rho}{4\pi}\int_\varphi\int_\theta d\theta d\varphi \sin\theta\left[\tau\frac{(\sin\theta\cos\varphi + \gamma\cos\theta)\cos\theta}{|\mathbf{\Lambda}\hat{\mathbf{n}}|}\right] \tag{6}$$

$$\sigma_{xx} = \frac{\rho}{4\pi}\int_\varphi\int_\theta d\theta d\varphi \sin\theta\left[\tau\frac{(\sin\theta\cos\varphi + \gamma\cos\theta)^2}{|\mathbf{\Lambda}\hat{\mathbf{n}}|}\right] \tag{7}$$

$$\sigma_{zz} = \frac{\rho}{4\pi}\int_\varphi\int_\theta d\theta d\varphi \sin\theta\left[\tau\frac{\cos^2\theta}{|\mathbf{\Lambda}\hat{\mathbf{n}}|}\right] \tag{8}$$

The integrals are taken over the ranges $0 \leq \theta \leq 2\pi$ and $0 \leq \varphi \leq \pi$. To compare with our results for the 3D FCC network, we use $\mu = 1$ and initial line density $\rho = \frac{12}{\sqrt{2}}$, corresponding to the fully-connected FCC lattice with $l_0 = 1$ [3].

We repeat the same process for the 2D case, in which the deformation tensor for simple shear is

$$\mathbf{\Lambda}(\gamma) = \begin{pmatrix} 1 & \gamma \\ 0 & 1 \end{pmatrix} \tag{9}$$

and the transformed orientation vector is

$$\mathbf{\Lambda}\hat{\mathbf{n}} = \begin{pmatrix} \cos\theta + \gamma\sin\theta \\ \sin\theta \end{pmatrix}. \tag{10}$$

The resulting components of the 2D stress tensor are calculated as follows:

$$\sigma_{xz} = \frac{\rho}{2\pi}\int_\theta d\theta\left[\tau\frac{(\cos\theta + \gamma\sin\theta)\sin\theta}{|\mathbf{\Lambda}\hat{\mathbf{n}}|}\right] \tag{11}$$

$$\sigma_{xx} = \frac{\rho}{2\pi}\int_\theta d\theta\left[\tau\frac{(\cos\theta + \gamma\sin\theta)^2}{|\mathbf{\Lambda}\hat{\mathbf{n}}|}\right] \tag{12}$$

$$\sigma_{zz} = \frac{\rho}{2\pi}\int_\theta d\theta\left[\tau\frac{\sin^2\theta}{|\mathbf{\Lambda}\hat{\mathbf{n}}|}\right] \tag{13}$$

Here, the integrals are taken over the range $0 \leq \theta \leq 2\pi$.

Principal strain axes for simple shear

For simple shear with deformation gradient tensor

$$\mathbf{\Lambda}(\gamma) = \begin{pmatrix} 1 & 0 & \gamma \\ 0 & 1 & 0 \\ 0 & 0 & 1 \end{pmatrix}, \tag{14}$$

we can decompose $\mathbf{\Lambda}$ into a combination of a pure stretch $\boldsymbol{U}$ and a rigid body rotation $\boldsymbol{R}$, satisfying $\mathbf{\Lambda} = \boldsymbol{R}\boldsymbol{U}$. From the right Cauchy-Green tensor $\boldsymbol{C} = \boldsymbol{U}^2 = \mathbf{\Lambda}^T\mathbf{\Lambda}$, we determine

$$\boldsymbol{U} = \frac{1}{\sqrt{4+\gamma^2}}\begin{pmatrix} 2 & 0 & \gamma \\ 0 & \sqrt{4+\gamma^2} & 0 \\ \gamma & 0 & 2+\gamma^2 \end{pmatrix}. \tag{15}$$

The eigenvalues of $\boldsymbol{U}$ are

$$\lambda_1 = \frac{\gamma + \sqrt{\gamma^2+4}}{2}, \quad \lambda_2 = \frac{-\gamma + \sqrt{\gamma^2+4}}{2}, \quad \lambda_3 = 1 \tag{16}$$

with corresponding eigenvectors

$$\boldsymbol{v}_1 = \left(\frac{1}{2}\left(-\gamma + \sqrt{4+\gamma^2}\right), 0, 1\right)$$

$$\boldsymbol{v}_2 = \left(\frac{1}{2}\left(-\gamma - \sqrt{4+\gamma^2}\right), 0, 1\right)$$

$$\boldsymbol{v}_3 = (0, 1, 0)$$

λ_1 and λ_2 correspond to the elongation l/l_0 along the axes of maximum extension and compression, respectively.

The rotation matrix $\boldsymbol{R}$ is determined as $\boldsymbol{R} = \boldsymbol{\Lambda}\boldsymbol{U}^{-1}$,

$$\boldsymbol{R} = \frac{1}{\sqrt{4+\gamma^2}} \begin{pmatrix} 2 & 0 & \gamma \\ 0 & \sqrt{4+\gamma^2} & 0 \\ -\gamma & 0 & 2 \end{pmatrix} \tag{17}$$

The maximum stretch direction then corresponds to $\boldsymbol{v}_1' = \boldsymbol{R}\boldsymbol{v}_1$. In the limit of small strains, $\boldsymbol{v}_1'$ is oriented at $\theta = \pi/4$ above the x-axis, in the x-z plane.

Bending interaction models

Prior work has shown that network models with bond-bending interactions (angle constraints between all nearest-neighbor bonds) exhibit the same strain-driven critical behavior as networks with freely-hinging crosslinks (angle constraints between only initially collinear nearest-neighbor bonds) [4, 5]. To emphasize that the details of the bending interactions do not influence our conclusions with regard to the normal stresses, we consider the mechanics of phantomized triangular networks with $z = 3.4$ and either freely-hinging crosslinks (bending along initially collinear fibers) or bond-bending interactions, both with $\tilde{\kappa} = 10^{-5}$. In Fig. S1, we show both K and the normal stresses σ_{ii}/γ^2 for each bending interaction type. We observe that the networks show qualitatively similar behavior in both cases, with $K \propto \tilde{\kappa}$ and $\sigma_{ii} \propto \tilde{\kappa}\gamma^2$ below the critical strain. The only apparent difference is that the magnitudes of K and the normal stresses are slightly higher for bond-bending networks than for networks with freely-hinging crosslinks in the bending-dominated regime. This is due to the additional angle constraints imposed by bond-bending interactions.

Packing-derived networks with varying connectivity

In Fig. S2, we show both $N_1/(\sigma_{xz}\gamma)$ and K for 2D packing-derived networks of size $W = 100$ with $\kappa = 10^{-5}$ and varying z. We observe that, for individual samples, peaks in $N_1/(\sigma_{xz}\gamma)$ occur at the z-dependent critical strain. On average, the Lodge-Meissner relation is satisfied.

[1] C. Storm, J. J. Pastore, F. C. MacKintosh, T. C. Lubensky, and P. A. Janmey, Nature **435**, 191 (2005).

[2] C. P. Broedersz, C. Storm, and F. C. MacKintosh, Physical Review E **79**, 1 (2009).

[3] A. J. Licup, A. Sharma, and F. C. MacKintosh, Physical Review E **93**, 1 (2016).

[4] A. Sharma, A. J. Licup, K. A. Jansen, R. Rens, M. Sheinman, G. H. Koenderink, and F. C. MacKintosh, Nature Physics **12**, 584 (2016).

[5] R. Rens, M. Vahabi, A. J. Licup, F. C. MacKintosh, and A. Sharma, Journal of Physical Chemistry B **120**, 5831 (2016).

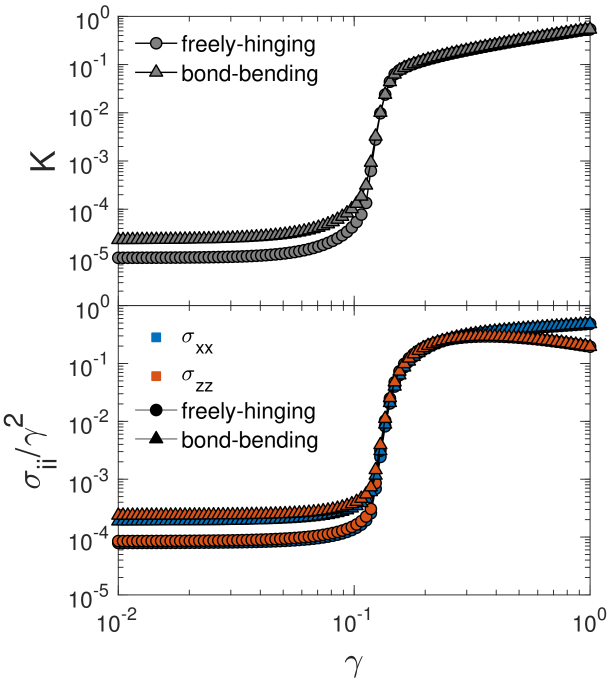

FIG. S1. Top: Differential shear modulus K vs. shear strain γ for 2D phantomized triangular networks with $z = 3.4$, $\tilde{\kappa} = 10^{-6}$ and $\delta_{\max} = 0.4$, with freely-hinging crosslinks and bending interactions only along fibers (triangles) and with bond-bending interactions between all nearest-neighbor bonds (circles). Bottom: Normal stresses σ_{xx} and σ_{zz}, both normalized by γ^2, as a function of γ for the same systems. Both K and σ_{ii} are higher in networks with bond-bending interactions than in the same networks with freely-hinging crosslinks, due to the additional angle constraints.

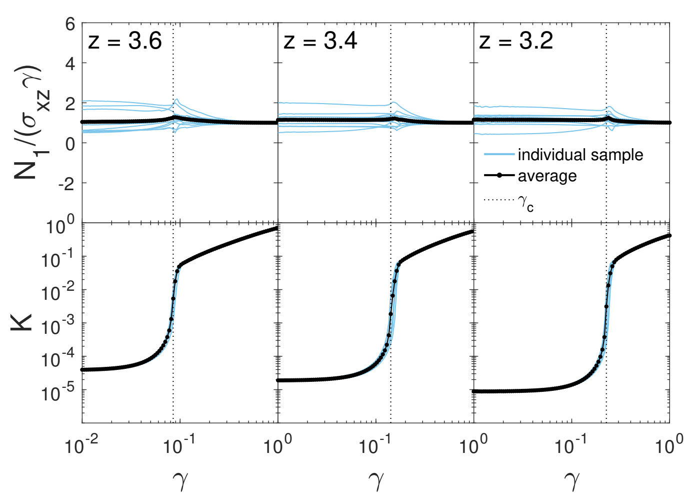

FIG. S2. In 2D packing-derived networks with $\kappa = 10^{-5}$ and varying z, we observe either upward or downward peaks in $N_1/(\sigma_{xz}\gamma)$ (top) for individual samples at the z-dependent critical strain γ_c, determined as the inflection point of K vs γ (bottom) plotted on a logarithmic scale. When the stress is averaged over all samples, the network ensemble approximately satisfies the Lodge-Meissner relation, such that $N_1/(\sigma_{xz}\gamma) = 1$ over the full strain range.